

## Two Novel Salen Based Chemosensors for Selective Recognition of Zinc(II) Ion

Longchao Du<sup>\*</sup>, Xiaoju Qin, Shixin Huang

School of Chemistry and Chemical Engineering & the Key Laboratory of Environment-friendly Polymer Materials of Anhui Province, Anhui University, Hefei, PRC

\*E-mail: [dulongchao@sina.com](mailto:dulongchao@sina.com)

Received: 16 May 2018 / Accepted: 20 June 2018 / Published: 5 August 2018

---

Two novel salen based chemosensors were synthesized and identified by FT-IR, <sup>1</sup>H-NMR and Elemental analysis. We evaluated the selectivity and sensitivity of probe L1 and L2 toward zinc ions via UV-vis, Cyclic voltammetry and <sup>1</sup>H-NMR measurement. The finding suggested the selective and sensitive recognition toward zinc ions was more typical than the other metal ions. The Zn<sup>2+</sup> can be detected well even the concentration of the probes are low to 10 μM. The stoichiometries of the complexes formed between the probes and Zn<sup>2+</sup> are 1:1, as determined by Job's method. And these probes showed distinctly different CV curves with Zn<sup>2+</sup>. <sup>1</sup>H-NMR research showed that the hydrogens in N=CH- and OH- are evidently up-field shift. These changes are due to the transform of N2O2 coordination plane of Schiff bases.

---

**Keywords:** Schiff base; Zinc ion; Chemosensor; Recognition

### 1. INTRODUCTION

Zinc is one of the essential trace elements in human body and endowed with the important role in human growth, reproduction, heredity, immunity, endocrine and other important physiological processes. The content of the required daily intake is very small, and zinc intake must be at a scientific equilibrium. If it is too much, can inhibit iron absorption and utilization, so as to cause iron deficiency anemia. However, excessive industrial emissions have broken the balance. Due to the serious impact of industrial pollution, the detection of metal ions has aroused widespread concern.

Recently, considerable attention has focused on the development of new artificial chemosensors for the recognition of physiologically and environmentally important analytes. Many mature methods has been exploited to detect the metal ions--atomic absorption spectrometry [1,2], inductively coupled

plasma emission spectrometry[3] and electrochemical methods[4-7], for example. However, the first two conditions are harsh, require expensive instruments[8], and the latter selectivity is poor[9].

A sensor that is simple, convenient, highly sensitive, low-cost, well-selective and easily prepared has long been desired. Salen ligands are versatile for metal complexation and a great deal of derivatives have been synthesised by varying N–N bridge and introducing substituents at the imine carbon or the aromatic ring. The salen based compounds can be used as probes for metal ion recognition due to their special conjugated structures and good chemical coordination properties[10-13]. In the reported literature, the salen based chemosensors can selectively identify some metal ions, such as  $Zn^{2+}$ [14-19],  $Al^{3+}$ [20-23],  $Ag^{+}$ [24],  $Cu^{2+}$ [25-27]. UV visible absorption spectrum has many advantages such as high sensitivity and easy operation, which is one of the most important identification methods.

Attributable to the current global environmental pollution, here, two novel salen based chemosensors was designed. They were expected to have great convenience and can be applied for the qualitative analysis and quantitative detection of zinc(II) ion in soil and wastewater faster and more efficiently.

## 2. EXPERIMENTAL

### 2.1. Materials and instrumentation

In a nitrogen-filled glove box, all manipulations for the preparation of salen ligand were performed using standard Schlenk techniques. Ethanol was dried using sodium and diethyl phthalate. The THF,  $CH_3CN$ ,  $CH_2Cl_2$  and cyclohexane were dried using  $CaH_2$  followed by vacuum transfer to a reservoir.

The Varian Mercury Plus 400 was used to record the  $^1H$ NMR (400 MHz). The Nicolet MAGNA-IR750 apparatus were used to obtain the Fourier transform infrared (FTIR) data via a thin film with the ratio of sample to KBr as 1: 100 by mass. The Fisons (Model EA 1108 CHNSO) was used to record the Elemental analyses. The Shimadzu UV-3600 spectrophotometer was used to measure the UV-vis absorption spectra. The electrochemical behaviors were investigated by three electrodes in 0.1M TBAP (tetrabutylammonium perchlorate)/ $CH_3CN$  solution. The working electrode is a glassy carbon electrode, the reference electrode is a silver/chloride silver electrode, and the counter electrode is a platinum wire electrode. The scanning rate was 0.1V / S.

### 2.2. Synthesis

#### *Synthesis of compound 1*

In a four-neck flash,  $AlCl_3$  (38.94g, 0.292mol) was added and dissolved in dry  $CH_2Cl_2$  (200mL). Then chloroacetyl chloride (32.90g, 0.291mol) and o-cresol (31.40g, 0.291mol) were added dropwise under  $N_2$ . The suspension was mixed for 24 hours. After completion of the reaction, the solution was extracted with  $CH_2Cl_2$  (3×50mL) and the collected organic layer was further dried over anhydrous

MgSO<sub>4</sub>. All of the solvent was removed in vacuo after the solution was filtered. Eluted with petroleum ether and ethyl acetate (V/V, 10:1), the obtained product was purified by column chromatography. The final product was collected as a gray white power. The yield was 12g (46.77%). IR (KBr): 3373 (OH), 1697 (C=O) cm<sup>-1</sup>. <sup>1</sup>H-NMR (CDCl<sub>3</sub>): δ 7.79 (s, 1H, m-H), 7.75 (d, J=8.4Hz, 1H, m-H), 6.84 (d, J=8.4Hz, 1H, o-H), 5.45 (s, 1H, Ar-OH), 4.65 (s, 2H, CH<sub>2</sub>), 2.30 (s, 3H, CH<sub>3</sub>) ppm.

#### *Synthesis of compound 2*

Compound 1 (10g, 0.054mol) was added to a one-neck flash and dissolved in trifluoroacetic acid (10mL). Then triethylsilane (6.24g, 0.054mol) was added. After the mixture was stirred for 12 hours, the pH value was adjusted to 8. After completion of the reaction, the solution was extracted with petroleum ether (3×50mL) and the collected organic layer was further dried over anhydrous MgSO<sub>4</sub>. All of the solvent was removed in vacuo after the solution was filtered. Eluted with petroleum ether and ethyl acetate (V/V, 10:1), the obtained product was purified by column chromatography. The final product was a light yellow oil. The yield was 6.9g (74.68%). IR (KBr): 3403 (OH) cm<sup>-1</sup>. <sup>1</sup>H-NMR (CDCl<sub>3</sub>): δ 6.96 (s, 1H, m-H), 6.91 (d, J=8.0Hz, 1H, m-H), 6.70 (d, J=8.1, 1H, o-H), 4.99 (s, 1H, Ar-OH), 3.65 (t, J=7.4Hz, 2H, CH<sub>2</sub>-Cl), 2.96 (t, J=7.4Hz, 2H, Ar-CH<sub>2</sub>), 2.23 (s, 3H, CH<sub>3</sub>) ppm.

#### *Synthesis of compound 3*

Compound 2 (6.00g, 0.352mol) was dissolved in THF (50mL). Magnesium chloride (13.43g, 0.141mol), triethylamine (14.98g, 0.148mol), and paraformaldehyde (4.23g, 0.141mol) were added under N<sub>2</sub>. The mixture was reacted at 80°C for 4 hours, after which the solvent was separated by a rotary evaporator. The solution was extracted with ethyl acetate (3×80mL) and the collected organic layer was further dried over anhydrous MgSO<sub>4</sub>. All of the solvent was removed in vacuo after the solution was filtered. Eluted with petroleum ether and ethyl acetate (V/V, 5:1), the obtained product was purified by column chromatography. The final product was a light yellow solid. The yield was 4.6g (65.90%). IR (KBr): 3462 (OH), 1639 (C=O) cm<sup>-1</sup>. <sup>1</sup>H-NMR (CDCl<sub>3</sub>): δ 11.18 (s, 1H, OH), 9.87 (s, 1H, CHO), 7.26 (s, 1H, m-H), 7.21 (s, 1H, m-H), 3.71 (t, J = 7.0Hz, 2H, CH<sub>2</sub>Cl), 3.03 (t, J = 7.3Hz, 2H, benzyl-CH<sub>2</sub>), 2.27 (s, 3H, CH<sub>3</sub>) ppm.

#### *Synthesis of compound 4*

Compound 3 (4.60g, 0.0232mol) was dissolved in THF (50mL) and NaI (3.47g, 0.0232mol) was put in. The mixture was reacted at 80°C for 24 hours and then cooled down to room temperature. The solution was extracted with CH<sub>2</sub>Cl<sub>2</sub> (3×50mL) and the collected organic layer was further dried over anhydrous MgSO<sub>4</sub>. All of the solvent was removed in vacuo after the solution was filtered. After eluted with petroleum ether and ethyl acetate (V/V, 5:1), the obtained product was purified by column chromatography. The final product was a light yellow solid. The yield was 5.4g (80.36%). IR (KBr): 3462 (OH), 1639 (CHO) cm<sup>-1</sup>. <sup>1</sup>H-NMR (CDCl<sub>3</sub>): δ 11.18 (s, 1H, OH), 9.87 (s, 1H, CHO), 7.26 (s, 1H, m-H), 7.21 (s, 1H, m-H), 3.34 (t, J = 7.5Hz, 2H, CH<sub>2</sub>I), 3.13 (t, J = 7.5Hz, 2H, benzyl-CH<sub>2</sub>), 2.27 (s, 3H, CH<sub>3</sub>) ppm.

*Synthesis of probe L1*

(1R,2R)-(-)-1,2-Diaminocyclohexane L-tartrate (1.41g, 0.00535mol) was dissolved in the 20mL saturated KOH aqueous solution. The solution was then extracted using CH<sub>2</sub>Cl<sub>2</sub>. The resulting solution and compound 4 (3.10g, 0.0107mol) were added to a flask combined with cyclohexane (50mL) under N<sub>2</sub>. The mixture was stirred under reflux for 24 hours and then cooled to room temperature. All of the solvent was removed in vacuo to give a yellow solid. The yield was 2.3g (65.71%). IR (KBr): 3432 (OH), 1639 (C=N) cm<sup>-1</sup>. <sup>1</sup>H-NMR (CDCl<sub>3</sub>): δ 13.45 (s, 2H, OH), 8.15 (s, 2H, N=CH-), 6.87 (s, 2H, m-H), 6.74 (d, J=1.7Hz, 2H, m-H), 3.24-3.22 (m, 2H, cyclohexyl-CH), 3.15 (t, J=7.6Hz, 4H, CH<sub>2</sub>I), 2.93 (t, J=7.8Hz, 4H, benzyl-CH<sub>2</sub>), 2.15 (s, 6H, CH<sub>3</sub>), 1.88-1.79 (m, 4H, cyclohexyl-CH<sub>2</sub>), 1.42-1.37 (m, 4H, cyclohexyl-CH<sub>2</sub>) ppm. Elemental analysis for C<sub>26</sub>H<sub>32</sub>O<sub>2</sub>N<sub>2</sub>I<sub>2</sub>: Calcd.: C, 47.43; H, 4.89; N, 4.25. Found, C, 47.84; H, 4.54; N, 4.72.

*Synthesis of compound 5*

The 4-Hydroxyphenethyl alcohol (5.150g, 0.0373mol), sodium hydroxide (8.981g, 0.224mol) and 50ml water were put into a flask, then chloroform (13.595g, 0.114mol) was added into. The reaction was carried out at 100°C for 24h. The solution was extracted with chloroform (3 × 25 mL) and the collected organic layer was further dried over anhydrous MgSO<sub>4</sub>. All of the solvent was removed in vacuo. The final product was a yellow oil. The yield was 4.422g (71.3%). IR (KBr) cm<sup>-1</sup>: 3403 (OH), 1653 (C=O). <sup>1</sup>H-NMR (CDCl<sub>3</sub>): δ 10.89 (s, 1H, Ar-OH), 9.86 (s, 1H, CHO) 7.42 (s, 1H, m-H), 7.39 (d, J = 8.5 Hz, 1H, o-H), 6.94 (d, J = 8.2 Hz, 1H, m-H), 3.87 (t, J = 6.1Hz, 2H, CH<sub>2</sub>), 2.86 (t, J = 6.6Hz, 2H, benzyl-CH<sub>2</sub>), 1.69 (s, 1H, phenemyl-OH).

*Synthesis of compound 6*

Compound 5 (4.422g, 0.0266mol), sulfoxide chloride (6.335g, 0.0532mol), dichloromethane 30ml were put into a flask. The reaction was carried out for 24h. After completion of the reaction, the solution was extracted with CH<sub>2</sub>Cl<sub>2</sub> (3×25mL) and the collected organic layer was further dried over anhydrous MgSO<sub>4</sub>. All of the solvent was removed in vacuo after the solution was filtered. The obtained product was purified by column chromatography. The yield was 1.982g(40.3%). IR (KBr) cm<sup>-1</sup>: 3427 (OH), 1653 (C=O), 653 (C-Cl). <sup>1</sup>H-NMR (CDCl<sub>3</sub>): δ 10.62 (s, 1H, Ar-OH), 10.24 (s, 1H, CHO), 7.56 (s, 1H, m-H), 7.44 (d, J = 8.5Hz, 1H, o-H), 6.96 (d, J = 8.4Hz, 1H, m-H), 3.81 (t, J = 6.9Hz, 2H, CH<sub>2</sub>Cl), 2.98 (t, J = 6.9Hz, 2H, benzyl-CH<sub>2</sub>).

*Synthesis of compound 7*

Compound 6 (1.982g, 0.0107mol) was dissolved in CH<sub>3</sub>CN (30mL) and NaI (4.812g, 0.0321mol) was put into. The mixture was reacted at 80°C for 24 hours. After completion of the reaction, water (30 mL) was added. The solution was extracted with CH<sub>2</sub>Cl<sub>2</sub> (3×10mL) and the collected organic layer was further dried over anhydrous MgSO<sub>4</sub>. All of the solvent was removed in vacuo after the solution was filtered. The obtained product was a clear yellow solid product without further purification. Yield was 2.883g (97.6%). IR (KBr) cm<sup>-1</sup>: 3444 (OH), 1656 (C=O), 488 (C-I); <sup>1</sup>H-NMR (CDCl<sub>3</sub>): δ 10.62 (s, 1H, Ar-OH), 10.24 (s, 1H, CHO), 7.53

(s, 1H, m-H) , 7.42 (d, J = 10.3Hz, 1H, o-H) , 6.94 (d, J = 8.4Hz, 1H, m-H) , 3.44 (t, J = 7.3Hz, 2H, CH<sub>2</sub>I) , 3.07 (t, J = 7.3Hz, 2H, benzyl-CH<sub>2</sub>) .

### Synthesis of probe L2

(1R,2R)-(-)-1,2-Diaminocyclohexane L-tartrate (0.775g, 0.00291mol) was dissolved in the 20mL saturated KOH aqueous solution. Subsequently, by CH<sub>2</sub>Cl<sub>2</sub>, the solution was extracted. The resulting solution and compound 7 (1.601g, 0.00581mol) were added with cyclohexane (50mL) to a flash. The mixture was reacted at room temperature for 24 hours. The reaction aggraded a light-yellow solid with 95.4% yield. IR (KBr) cm<sup>-1</sup>: 3424 (OH) , 2137 (C=N) 1632 (C=O) , 479 (C-I) ; <sup>1</sup>H-NMR(CDCl<sub>3</sub>): δ 13.21 (s, 2H, Ar-OH) , 8.21 (s, 2H, N=CH-) , 7.05 (d, J=8.1Hz, 2H, m-H) , 6.96 (d, J=8.5Hz, 2H, o-H) , 6.84 (d, J = 8.4Hz, 2H, m-H) , 3.36~3.31 (m, 2H, cyclohexyl-CH) , 3.23 (t, J=7.6Hz, 4H, CH<sub>2</sub>I) , 3.03 (t, J=7.7Hz, 4H, benzyl-CH<sub>2</sub>) , 1.97~1.87 (m, 4H, cyclohexyl-CH<sub>2</sub>), 1.52~1.45(m, 4H, cyclohexyl-CH<sub>2</sub>). Elemental analysis for C<sub>24</sub>H<sub>28</sub>O<sub>2</sub>N<sub>2</sub>I<sub>2</sub>: Calcd.: C, 45.73; H, 4.48; N, 4.44. Found, C, 45.92; H, 4.13; N, 4.68.

### 2.3. Analysis

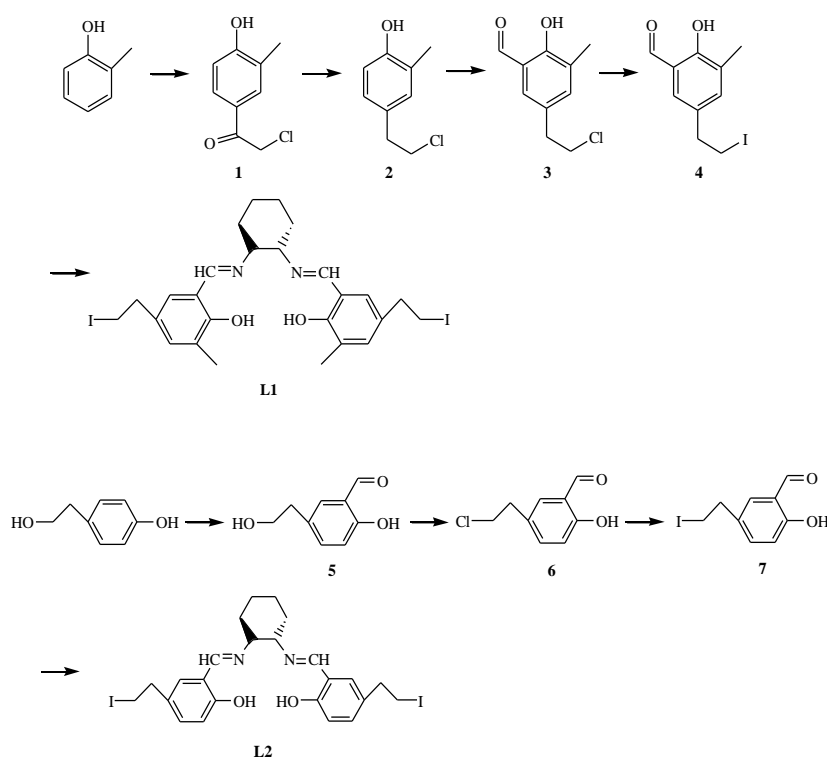
Na<sup>+</sup>, K<sup>+</sup>, Mg<sup>2+</sup>, Al<sup>3+</sup>, Fe<sup>3+</sup>, Zn<sup>2+</sup>, Ag<sup>+</sup>, Pb<sup>2+</sup>, Co<sup>2+</sup>, Li<sup>+</sup>, Ba<sup>2+</sup>, Ni<sup>2+</sup>, Ca<sup>2+</sup>, Cd<sup>2+</sup>, La<sup>3+</sup>, Cu<sup>2+</sup> and Mn<sup>2+</sup> are prepared from their nitrates. A stock solution of L1 and L2 (1 mM) was prepared by DMF. By placing 30 μL of the probe stock solution in a cuvette, adding appropriate aliquots of each ionic stock solution, and diluting the solution to 3 mL with DMF, a test solution was prepared.

## 3. RESULTS AND DISCUSSION

Scheme 1 is the synthetic route for sensors L1 and L2. Both of these sensors were purified and characterized using spectroscopic and elemental analysis. By <sup>1</sup>H NMR, the intermediate was characterized and displayed in supporting information. Using UV-vis absorption spectroscopy, the probe L1 was investigated in presence of those metal ions (Na<sup>+</sup>, K<sup>+</sup>, Mg<sup>2+</sup>, Al<sup>3+</sup>, Fe<sup>3+</sup>, Zn<sup>2+</sup>, Ag<sup>+</sup>, Pb<sup>2+</sup>, Co<sup>2+</sup>, Li<sup>+</sup>, Ba<sup>2+</sup>, Ni<sup>2+</sup>, Ca<sup>2+</sup>, Cd<sup>2+</sup>, La<sup>3+</sup>, Cu<sup>2+</sup>, Mn<sup>2+</sup>). As shown in Fig. 1, the free probe L1 shows a 330nm centered absorption band. After adding 1.0 equivalent Zn<sup>2+</sup> to the probe L1, a new absorption band was observed with center at 370nm, while that of 330nm band for free probe L1 disappeared. It can be seen that the spectral changes is occurring by the process of intramolecular charge transfer (ICT) [28]. However, there have few absorption changes at the addition of other metal ions to the probe L1. This is probably because the size, charge and electronic configuration of Zn<sup>2+</sup> and probe L1 are very suitable for forming metal complexes with each other compared with other metal ions. The results suggest that the probe L1 has good selectivity for Zn<sup>2+</sup>.

Similar phenomena occur in other salen probes research. In the study[29], when 1.0 equiv of Zn<sup>2+</sup> ion was added, there was a 5.6-fold remarkable enhancement in the fluorescence emission intensity for their salen probe, and at the same time accompanied by a slight red shift. For other

cations, slight increase or quenching can be detected. In like manner, at the research of input logic gates using salen based organic nanoparticles (ONPs) chemosensor to detect  $Zn^{2+}$  and  $Al^{3+}$  ions in aqueous medium [30], the results show that the increasing  $Zn^{2+}$  ions concentration can rise obviously the fluorescence intensity, proving that  $Zn^{2+}$  ions can be detected efficiently by salen-ONPs as chemosensor. Further more, the system of salen-ONPs/ $Zn^{2+}$  act as an ON-OFF switch when the pH is 6.0 to 4.0. Although salen-ONPs/ $Al^{3+}$  has no effect on the fluorescence spectrum, when  $Al^{3+}$  ions are added to salen-ONPs/ $Zn^{2+}$  system, the highest fluorescence intensity is observed (order  $Zn^{2+}$  to salen-ONPs, followed by  $Al^{3+}$ ). These are all the same due to the formation of a bond between the  $Zn^{2+}$  ion and ligand, which enhances the fluorescence emission of salen-ONPs. These results are consistent with our research.



**Scheme 1.** Synthetic route of probe L1 and L2.

When different amounts of  $Zn^{2+}$  was added to the probe L1, the 370nm absorption band increases gradually, and the primary 330nm absorption band decreased gradually as the  $Zn^{2+}$  concentration increased (Fig. 2). After 1.0 equiv  $Zn^{2+}$  added, the absorbance at 370 nm reached the peak value, indicating that the 1:1 bond mode between chemical sensor and  $Zn^{2+}$  was formed (Fig. 3). The same situation occurs also in the study[31]. When their probe reacted with  $Zn^{2+}$  ion, the Job's plot shows that a 1 to 1 stoichiometric ligand-metal binding happens and the fluorescence intensity achieves the maximum when the molar fraction of their probe is 0.5. These confirm the chelation mode between the probe and  $Zn^{2+}$  ion.

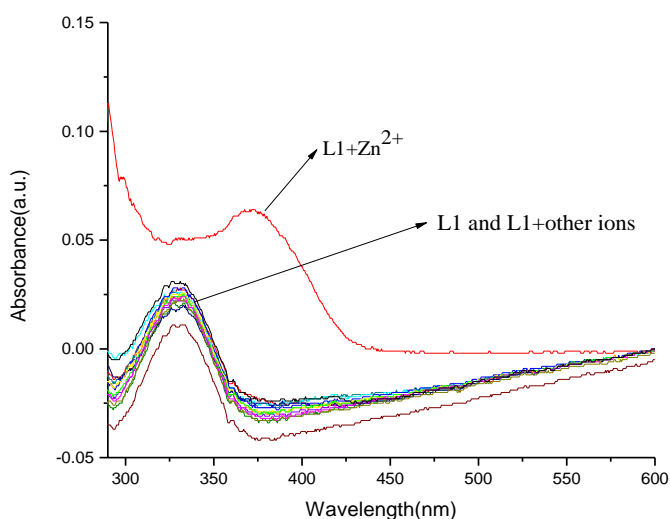


**Figure 1.** UV-vis absorption of probe L1 (10  $\mu\text{M}$ ) upon addition of different metal ions in DMF:  $\text{Zn}^{2+}$ ,  $\text{Li}^+$ ,  $\text{Na}^+$ ,  $\text{K}^+$ ,  $\text{Ag}^+$ ,  $\text{Mg}^{2+}$ ,  $\text{Cd}^{2+}$ ,  $\text{Mn}^{2+}$ ,  $\text{Al}^{3+}$ ,  $\text{Cu}^{2+}$ ,  $\text{Fe}^{3+}$ ,  $\text{Pb}^{2+}$ ,  $\text{Co}^{2+}$ ,  $\text{Ba}^{2+}$ ,  $\text{Ni}^{2+}$ ,  $\text{Ca}^{2+}$ ,  $\text{La}^{3+}$  (1.0 equiv).

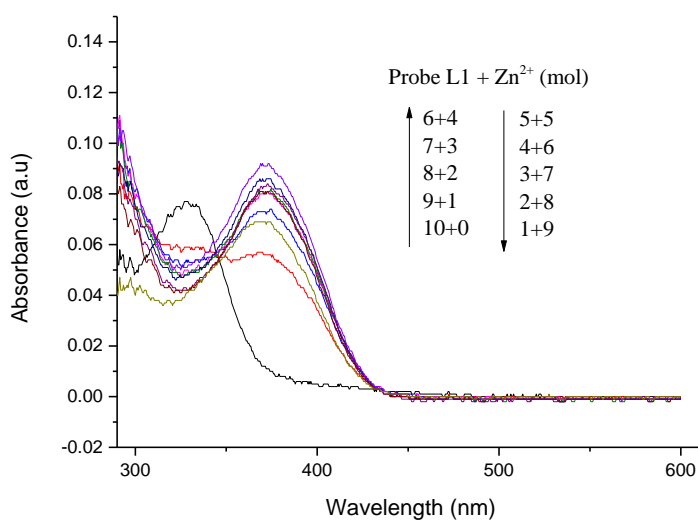


**Figure 2.** The changes of absorption spectrum (290-600nm) for gradual addition of  $\text{Zn}^{2+}$  upon L1 (10  $\mu\text{M}$ ) in DMF solution.

In the presence of different metal ions, the probe L2 was also studied by UV-visible absorption. As shown in Fig. 4, there has a major absorption band centered at 325nm for the free probe L2, which is 5nm lower than that of L1. This may be due to the lack of a methyl group in the phenyl ring. A new absorption band was observed at 370nm and the band at 325nm for free probe L2 disappeared by adding 1.0 equivalent  $\text{Zn}^{2+}$ . However, adding other metal ions to detect L2 has no absorption changes. This may also be that the size, charge and electronic configuration of  $\text{Zn}^{2+}$  and probe L2 are very suitable for the formation of metal complexes compared with other metal ions. These results indicate that the selectivity of probe L2 for  $\text{Zn}^{2+}$  is also high. It is consistent with L1. This may be that the

structure of the two probes is almost unchanged, and the presence of methyl groups on the phenyl ring does not affect their recognition of metal ions

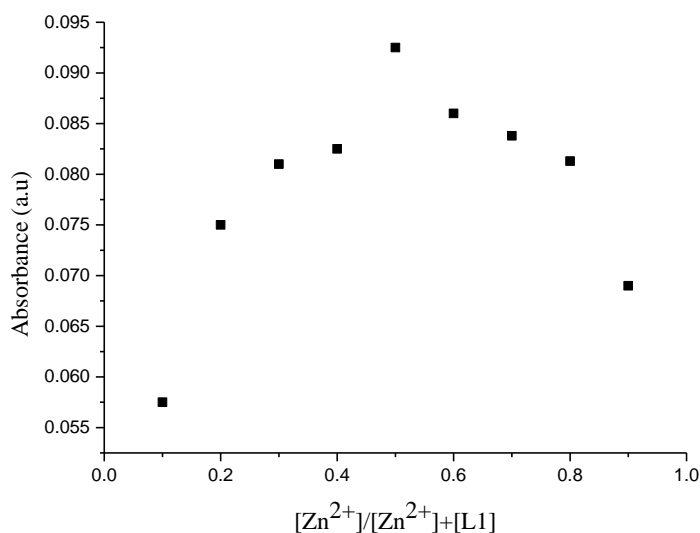


**Figure 3.** Job's plot of probe L1 to Zn<sup>2+</sup>, the absorbance of 370 nm was plotted for mole fraction of Zn<sup>2+</sup>. The initial concentration of L1 is 10 μM.

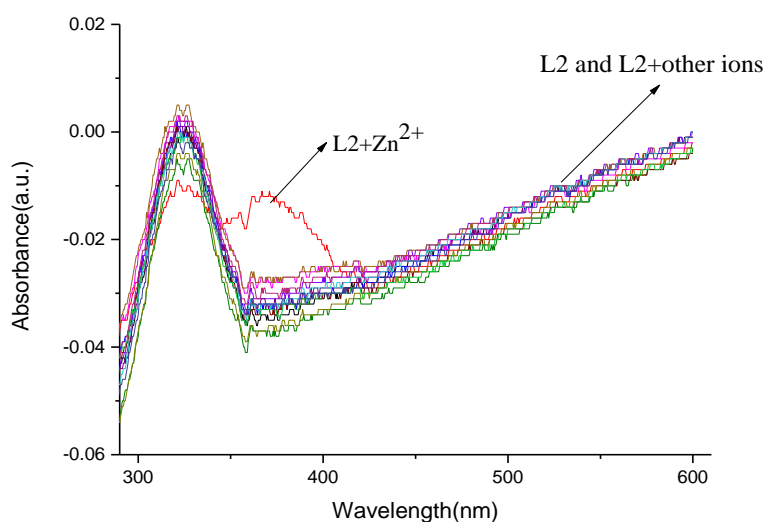


**Figure 4.** UV-vis absorption of probe L2 (10 μM) upon addition of different metal ions in DMF: Zn<sup>2+</sup>, Li<sup>+</sup>, Na<sup>+</sup>, K<sup>+</sup>, Ag<sup>+</sup>, Mg<sup>2+</sup>, Cd<sup>2+</sup>, Mn<sup>2+</sup>, Al<sup>3+</sup>, Cu<sup>2+</sup>, Fe<sup>3+</sup>, Pb<sup>2+</sup>, Co<sup>2+</sup>, Ba<sup>2+</sup>, Ni<sup>2+</sup>, Ca<sup>2+</sup>, La<sup>3+</sup> (1.0 equiv).

As different amounts of Zn<sup>2+</sup> were added to the probe L2, the centered at 370nm strong absorption band increases gradually, while the main 325nm absorption bands for ligand decrease gradually as the Zn<sup>2+</sup> concentration increased (Fig 5). When 1.0 equiv Zn<sup>2+</sup> was added, the absorbance



at 370nm peaked, suggesting that a 1:1 bond pattern was formed between the chemical sensor and  $Zn^{2+}$  (Fig. 6), as that of L1 and  $Zn^{2+}$ . At the same time, it can be seen that  $Zn^{2+}$  can be well detected even when the probe concentration is as low as  $10\mu M$ . All of these UV-visible absorption tests and Job's plots showed that the probe L1 and L2 had the identical  $Zn^{2+}$  ion recognition ability and the chelation mode were 1:1 for both these probes and  $Zn^{2+}$  ion.

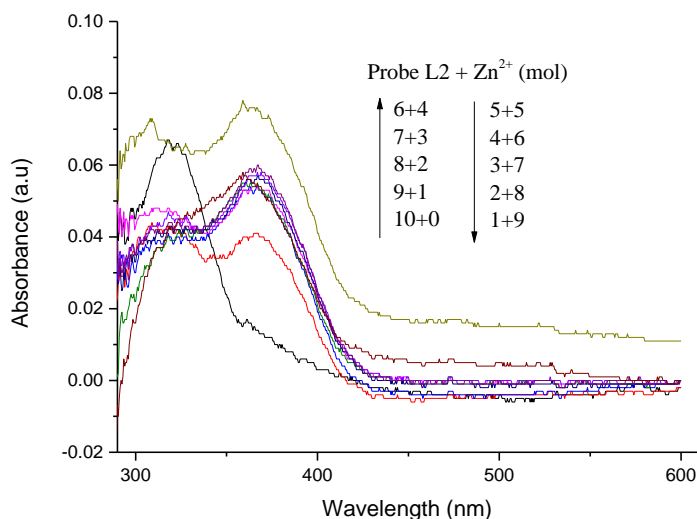


**Figure 5.** The changes of absorption spectrum (290-600nm) for gradual addition of  $Zn^{2+}$  upon L2 ( $10\mu M$ ) in DMF solution.

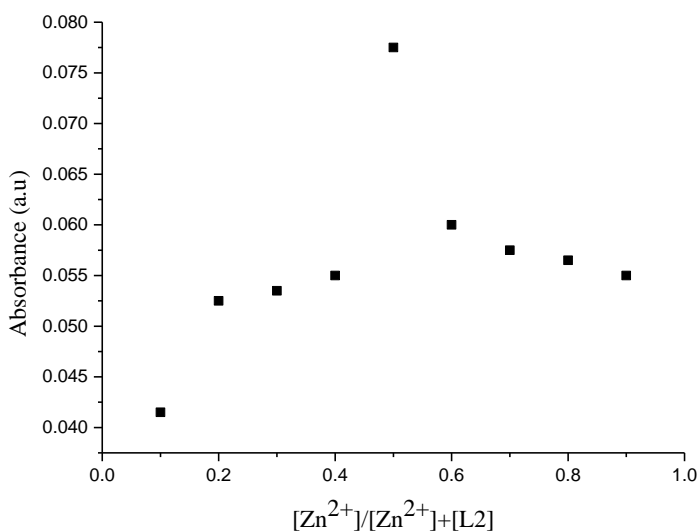


**Figure 6.** Job's plot of probe L2 to  $Zn^{2+}$ , the absorbance of 370 nm was plotted for mole fraction of  $Zn^{2+}$ . The initial concentration of L1 is  $10\mu M$ .

In order to have a further understanding of sensing behavior of the L1 and L2 toward  $Zn^{2+}$  ion, electrochemical investigation were performed by employing cyclic voltammetry (CV). Firstly, the electrochemical behaviors of L1 and L2 were investigated in 0.1M TBAP (tetrabutylammonium

perchlorate)/CH<sub>3</sub>CN solution. The scanning rate was 0.1V / S. Fig. 7 (a) showed that the sensor L1 has an oxidation peak ( $E_{pa} = -0.749\text{V}$ ) and a reduction peak ( $E_{pc} = 1.078\text{V}$ ) in  $-1.2$  to  $1.6$  V potential range. After L1 interacted with  $\text{Zn}^{2+}$  ions at 1.0 equiv, it showed distinctly different CV curve. The oxidation peak of  $\text{L1} + \text{Zn}^{2+}$  appears at  $-0.701\text{V}$ , despite the reduction peak is still at  $1.078\text{V}$ . These changes can be that the sensor L1 coordinated with  $\text{Zn}^{2+}$  ion through the  $\text{N}_2\text{O}_2$  coordination plane of Schiff bases, which indicated the formation of  $\text{L1-Zn(II)}$  complex. And so the oxidation peak of L1 changes from  $-0.749\text{V}$  to  $-0.701\text{V}$ .

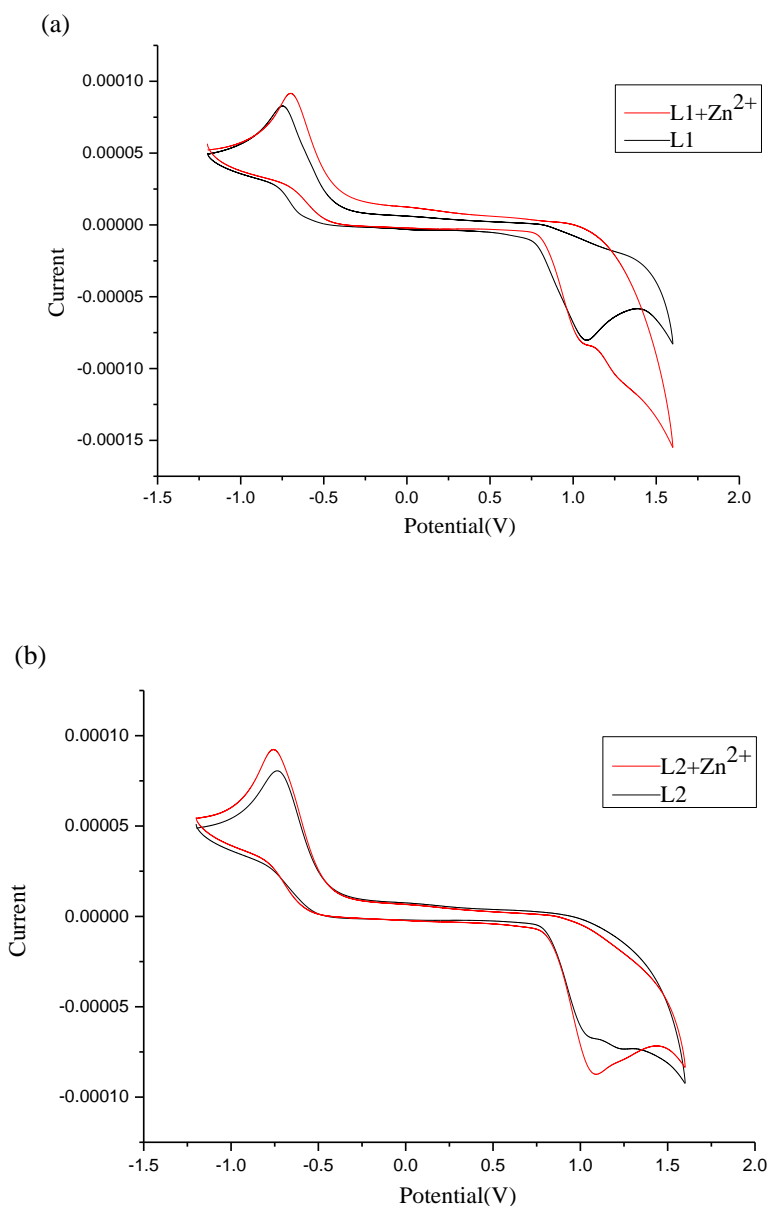


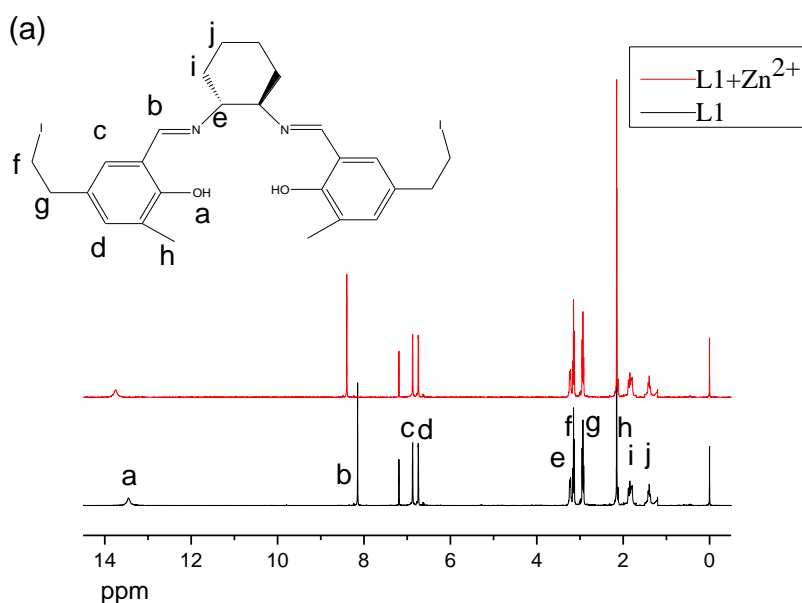
**Figure 7.** CV profile of (a) L1 and after complexation with  $\text{Zn}^{2+}$ , (b) L2 and after complexation with  $\text{Zn}^{2+}$  at 1.0 equiv. The concentration of L1/L2 is  $10\ \mu\text{M}$ .

As shown in Fig. 7(b), L2 has one oxidation peak ( $E_{pa} = -0.742\text{V}$ ) and two reduction peaks

( $E_{pc1}= 1.077V$ ,  $E_{pc2}= 1.232V$ ). When the  $Zn^{2+}$  ion was added at 1.0 equivalent, the oxidation peak was shifted to  $-0.763V$  and there was only one reduction peak ( $E_{pc1}= 1.087V$ ) for  $L2+Zn^{2+}$ . Similarly, we can come to conclude that L2 can also form complex with  $Zn^{2+}$  ion. All these observations revealed that the sensors L1 and L2 can sensitively recognize  $Zn^{2+}$  ion. Similarity, Singh et al. [32] authenticated the binding of their sensors with  $Fe^{3+}$  ion by CV profiles. By stepwise titration addition of  $Fe^{3+}$  ion, the fluorescence intensity of emission peaks of their sensors decrease stepwise. When the concentration of  $Fe^{3+}$  ion increases from  $0\mu M$  to  $1000\mu M$ , the emission peaks were quenched finally.

Further more, the binding mode of ligand and  $Zn^{2+}$  was also determined by  $^1H$ -NMR spectroscopy. After adding 1.0 equivalent  $Zn^{2+}$ , the  $^1H$ -NMR spectra of L1 and L2 are recorded in  $CDCl_3$ . As shown in Fig. 8, the apparent spectral changes were found. After  $Zn^{2+}$  addition, hydrogen in both OH- and N = CH- undergoes up-field shifts for L1 and L2. For the L1, the hydrogen in N=CH- up-field shifted from  $\delta 8.15$  to  $\delta 8.40$ , and the hydrogen in OH- up-field shifted from  $\delta 13.45$  to  $\delta 13.74$ . For the L2, the hydrogen in N=CH- up-field shifted from  $\delta 8.21$  to  $\delta 8.44$ , and the hydrogen in OH- up-field shifted from  $\delta 13.21$  to  $\delta 13.51$ . The signals of other protons were almost constant. These changes are also due to the transform of N2O2 coordination plane of Schiff bases, which authenticated the probe L1 and L2 already coordinate with  $Zn^{2+}$ . Analogously, in the study of cage-like tris(salen)-type metallocryptand for cooperative guest recognition [33], the guest recognition behavior of  $H_6L$  and the metallohost  $[LZn_3]$  was investigated by  $^1H$ -NMR titration experiments in  $CDCl_3/DMSO-d_6$  (9:1). The study found that different alkali earth metal ions can produce different shifts in  $^1H$ -NMR for their metallohost  $[LZn_3]$ .

By analyzing the results of UV-vis, electrochemical and  $^1H$ -NMR studies, Scheme 2 shows the possible binding modes of ligand and  $Zn^{2+}$ . For the complex, the metal ion can be linked to two oxygen atoms and two nitrogen atoms of the phenolic and imine groups, and the coordination number of  $Zn^{2+}$  ion is 4.



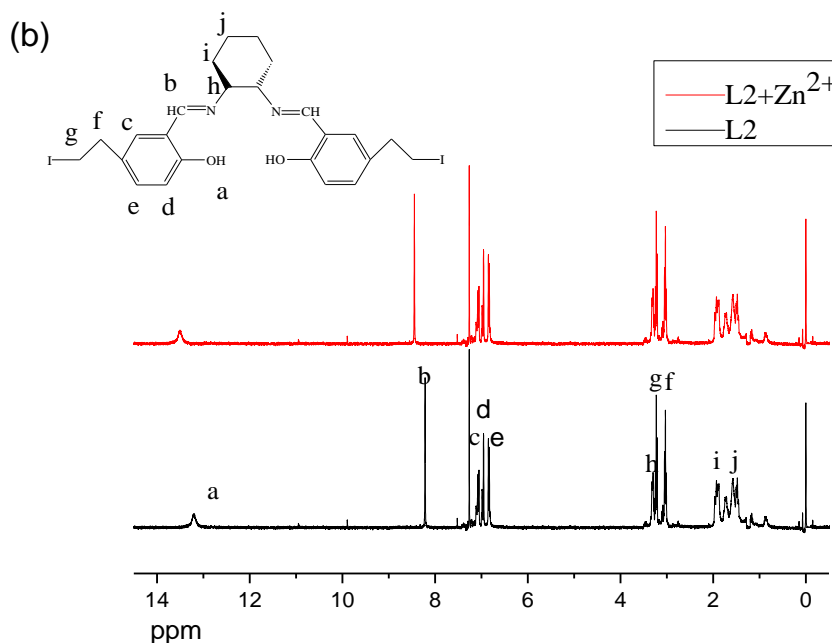
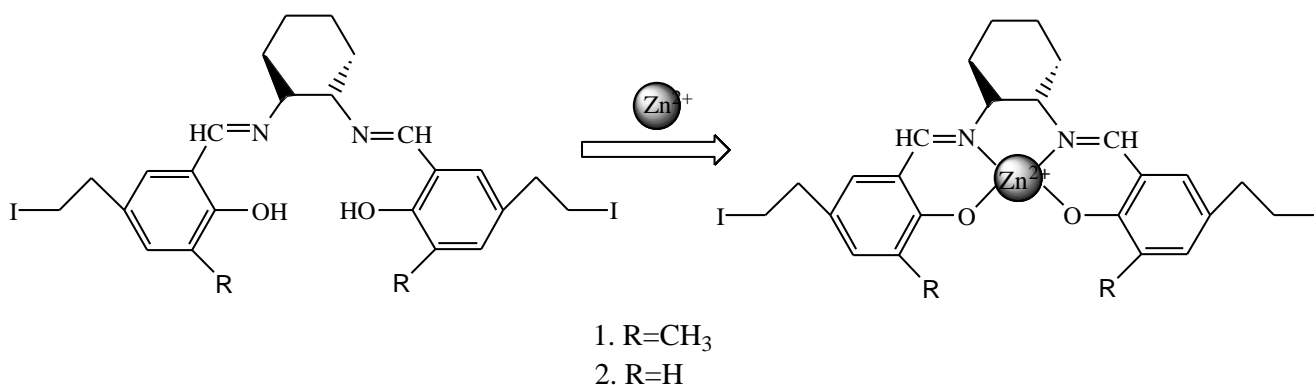


**Figure 8.**  $^1\text{H-NMR}$  spectra for (a) L1 / (b) L2 with  $\text{Zn}^{2+}$  at 1.0 equiv in  $\text{CDCl}_3$ .



**Scheme 2.** Schematic diagram of  $\text{Zn}^{2+}$ /probe binding mode.

#### 4. CONCLUSION

In summary, two new salen-based  $\text{Zn}^{2+}$  ion chemical sensors have developed. They show higher selectivity and sensitivity to  $\text{Zn}^{2+}$  than other metal ions. The  $\text{Zn}^{2+}$  can be detected well even the concentration of the probes are low to  $10\ \mu\text{M}$ . The stoichiometries of the complexes formed between the probes and  $\text{Zn}^{2+}$  are 1:1, as determined by Job's method. And these probes showed distinctly different CV curves when equivalent  $\text{Zn}^{2+}$  was added.  $^1\text{H-NMR}$  research showed that the hydrogens in  $\text{N}=\text{CH}$ - and  $\text{OH}$ - are evidently up-field shift. These changes are due to the transform of  $\text{N}_2\text{O}_2$  coordination plane of Schiff bases.

SUPPORTING MATERIAL:

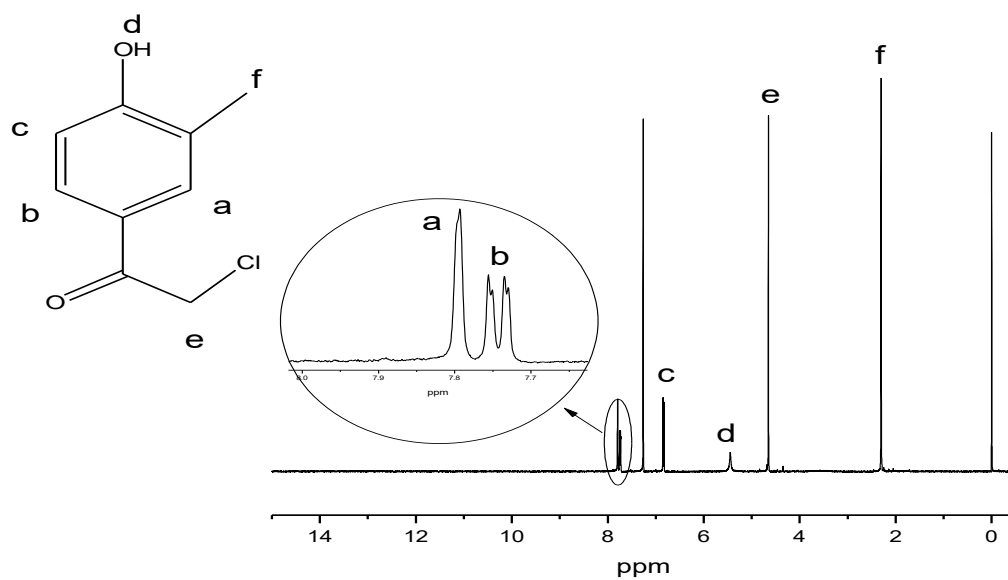


Fig. S1. <sup>1</sup>H NMR spectrum of the compound 1 in CDCl<sub>3</sub>

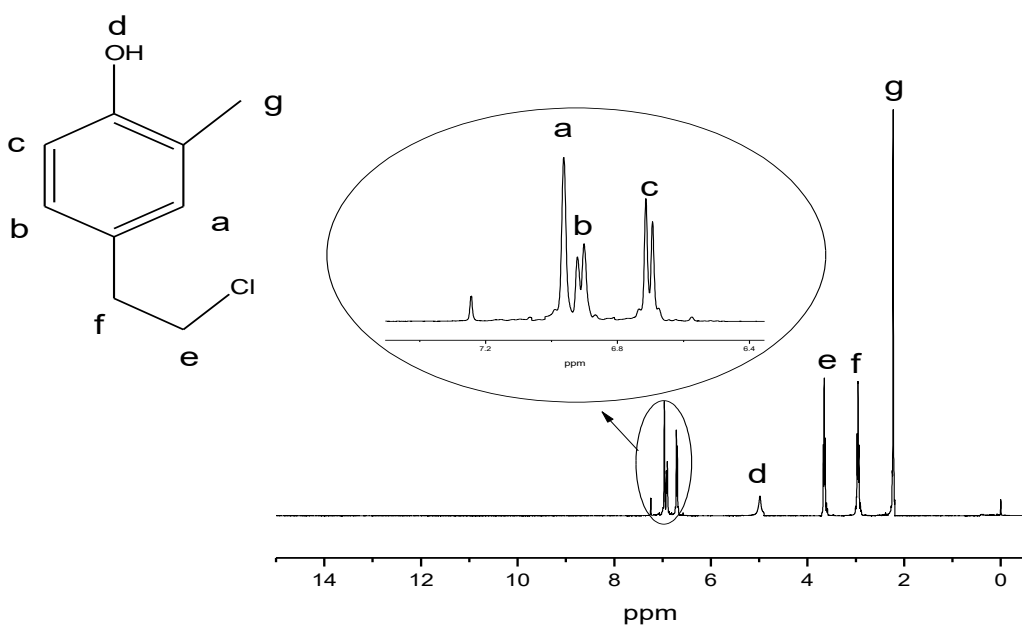
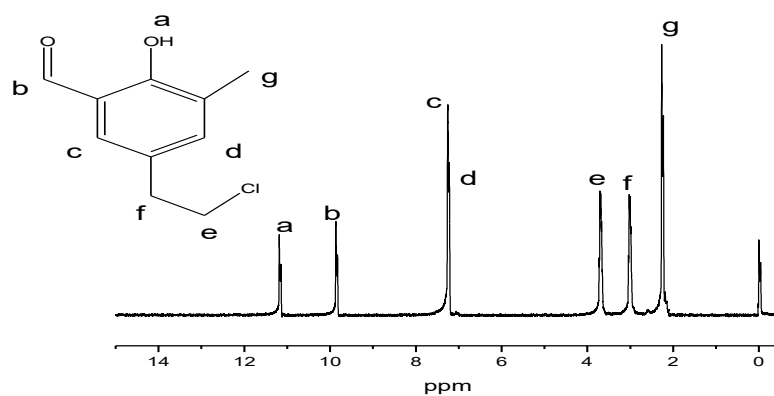
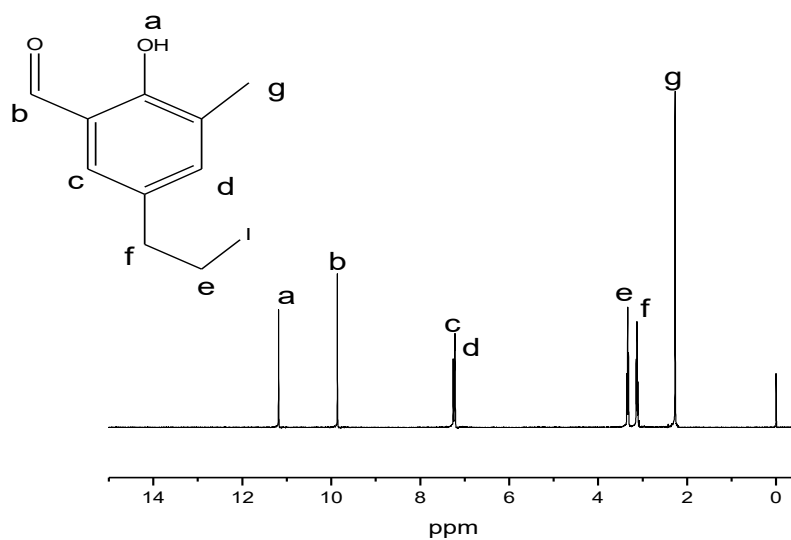


Fig. S2. <sup>1</sup>H NMR spectrum of the compound 2 in CDCl<sub>3</sub>



**Fig. S3.**  $^1\text{H}$  NMR spectrum of the compound 3 in  $\text{CDCl}_3$



**Fig. S4.**  $^1\text{H}$  NMR spectrum of the compound 4 in  $\text{CDCl}_3$

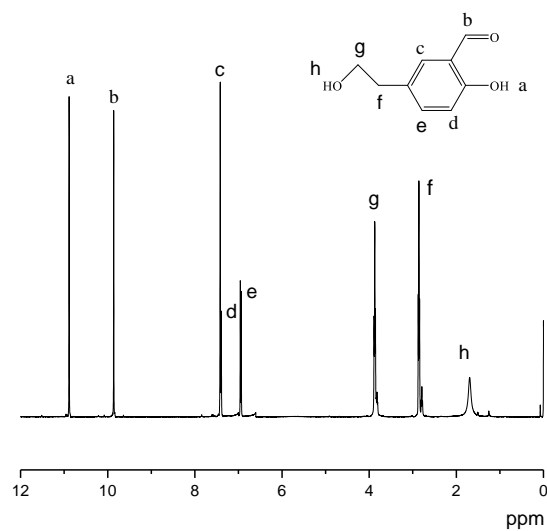


**Fig. S5.**  $^1\text{H}$  NMR spectrum of the compound 5 in  $\text{CDCl}_3$ .

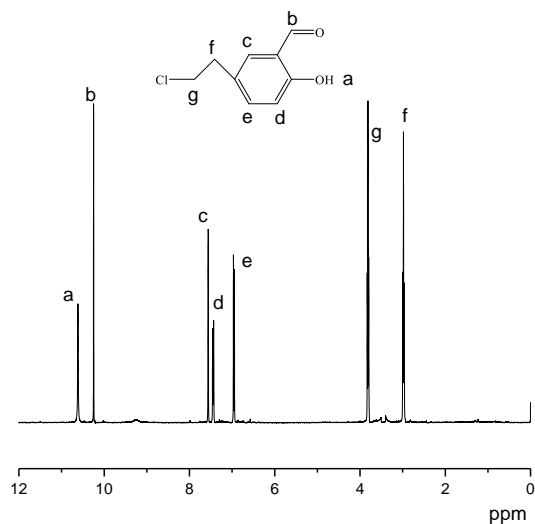


**Fig. S6.**  $^1\text{H}$  NMR spectrum of the compound 6 in  $\text{CDCl}_3$ .

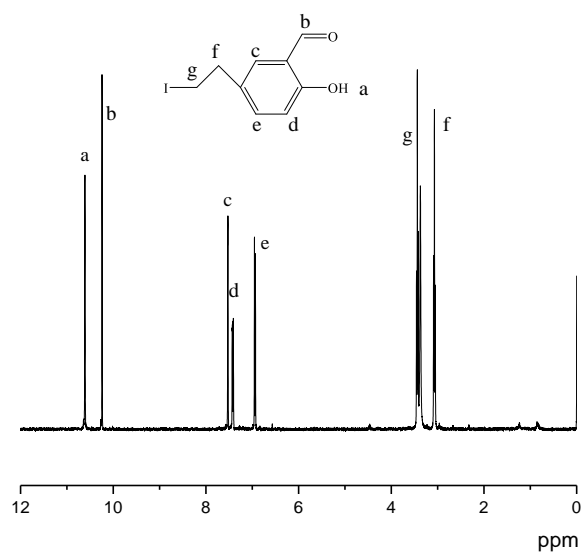


**Fig.S7.**  $^1\text{H}$  NMR spectrum of the compound 7 in  $\text{CDCl}_3$ .

#### ACKNOWLEDGEMENTS

The financial support from the 211 Project of Anhui University (J04100301) and Anhui Province Key Laboratory of Environment-friendly Polymer Materials are thanked by the authors.

#### References

1. M.A. Kamyabi and A. Aghaei, *Spectrochim. Acta. B.*, 128 (2017) 17.
2. B. Gómez-Nieto, M.J. Gismera, M.T. Sevilla and J.R. Procopio, *Food. Chem.*, 219 (2017) 69.
3. V. Topalidis, A. Harris, C.J. Hardaway, G. Benipal and C. Douvris, *Microchem. J.*, 130 (2017) 213.
4. J. Hoyos-Arbeláez, M. Vázquez and J. Contreras-Calderón, *Food. Chem.*, 221 (2017) 1371.
5. Y. Liu, J. Hu, Q. Teng and H. Zhang, *Sensor. Actuat. B-chem.*, 238 (2017) 166.
6. T. Liu, J. Yin, Y. Wang and P. Miao, *J. Electroanal. Chem.*, 783 (2016) 304.

7. F. Tan, L. Cong, N.M. Saucedo, J. Gao, X. Li and A. Mulchandani, *J. Hazard. Mater.*, 320 (2016) 226.
8. P. Donato, F. Cacciola, P.Q. Tranchida, P. Dugo and L. Mondello, *Mass. Spec. Rev.*, 31 (2012) 523.
9. Z. Guo, Y. Wei, R. Yang, J. Liu and X. Huang, *Electrochim. Acta.*, 87 (2013) 46.
10. Y. Han, J. Sun, G. Wang and C. Yan, *J. Mol. Struct.*, 1083 (2015) 300.
11. S. Zhang, Q. Niu, L. Lan and T. Li, *Sensor. Actuat. B-chem.*, 240 (2017) 793.
12. D. Peralta-Domínguez, M. Rodríguez, G. Ramos-Ortíz, J. Maldonado, M.A. Meneses-Nava, O. Barbosa-García, R. Santillan and N. FarfáncaCentro, *Sensor. Actuat. B-chem.*, 207 (2015) 511.
13. X. Wang, H. Wang and S. Feng, *Sensor. Actuat. B.*, 241 (2017) 65.
14. M. Kumar, A. Kumar, M.K. Singh, S.K. Sahu and R.P. John, *Sensor. Actuat. B.*, 241 (2017) 1218.
15. M. Yang, Y. Zhang, W. Zhu, H. Wang, J. Huang, L. Cheng, H. Zhou, J. Wu and Y. Tian, *J. Mater. Chem. C.*, 3 (2015) 1994.
16. N. Zhang, X. Tian, J. Zheng, X. Zhang, W. Zhu, Y. Tian, Q. Zhu and H. Zhou, *Dyes. Pigments.*, 124 (2016) 174.
17. J. Zhu, Y. Zhang, Y. Chen, T. Sun, Y. Tang, Y. Huang, Q. Yang, D. Ma, Y. Wang and M. Wang, *Tetrahedron. Lett.*, 58 (2017) 365.
18. J. Yan, L. Fan, J. Qin, C. Li and Z. Yang, *Tetrahedron. Lett.*, 57 (2016) 2910.
19. C. Patra, A.K. Bhanja, C. Sen, D. Ojha, D. Chattopadhyay, A. Mahapatra and C. Sinh, *Sensor. Actuat. B-chem.*, 228 (2016) 287.
20. N. Yin, H. Diao, W. Liu, J. Wang and L. Feng, *Spectrochim. Acta. A.*, 153 (2016) 1.
21. J. Qin and Z. Yang, *J. Photoch. Photobio. A.*, 303 (2015) 99.
22. V.K. Gupta, A.K. Singh and N. Mergu, *Electrochim. Acta.*, 117 (2014) 405.
23. K. Zhang, Z. Yang, B. Wang, S. Sun, Y. Li, T. Li, Z. Liu and J. An, *Spectrochim. Acta. A.*, 124 (2014) 59.
24. H.H. Hammud, S.E. Shazly, G. Sonji, N. Sonji and K.H. Bouhadir, *Spectrochim. Acta. A.*, 150 (2015) 94.
25. X. Wang, T. Xu and H. Duan, *Sensor. Actuat. B.*, 214 (2015) 138.
26. K. Wang, W. Feng, Y. Wang, D. Cao, R. Guan, X. Yu and Q. Wu, *Inorg. Chem. Comm.*, 71 (2016) 102.
27. X. Ge, J. Pi, W. Zhu, X. Gan, J. Zheng, X. Tang, Y. Yang, H. Zhou, J. Wu and Y. Tian, *Spectrochim. Acta. A.*, 151 (2015) 390.
28. N. Mergu and V.K. Gupta, *Sensor. Actuat. B.*, 210 (2015) 408.
29. J.D. Wu, X. Zhao, Y.X. Gao, J. Hu and Y. Ju, *Sensor. Actuat. B.*, 221 (2015) 334.
30. C.A. Huerta-Aguilar, T. Pandiyan, N. Singh and N. Jayanthi, *Spectrochim. Acta. A.*, 146 (2015) 142.
31. H. Yu, T. Yu, M.T. Sun, J. Sun, S. Zhang, S.H. Wang and H. Jiang, *Talanta*, 125 (2014) 301.
32. T. Raj, P. Saluja and N. Singh, *Sensor. Actuat. B.*, 206 (2015) 98.
33. S. Akine, S.J. Piao, M. Miyashita and T. Nabeshima, *Tetrahedron. Lett.*, 54 (2013) 6541.